Research Article

Human-Trust Based Feedback Control (HTBFC) Five-Dimensional Manifold Info-Geometric Analysis and how HTBEC Impacts Robotics

Ismail A Mageed*

Member IEEE, IAENG

*Corresponding Author
Ismail A Mageed, Member IEEE, IAENG

Abstract
This work examines the five-dimensional HTBFC Manifold's info-geometrics using effective information geometry (IG) techniques. The performance of HTBFC can be analysed from a novel relativistic approach by merging IG framework. Subcases of manifolds in two and three dimensions are studied. Human-machine interactions (HMIs) can now be unified through IG in a novel way because to this study. The presentation includes the essential robotic applications of HTBFC. A few newly identified unsolved issues and suggestions for additional study are included in the conclusions.

Keywords: Human- Machine Interactions (HMIs), Human-Trust Based Feedback Control (HTBFC), Robotics.

1. Introduction

Information geometry (IG) is a state-of-the-art geometric methodology that looks at both model analysis and geometry visualization from an IG standpoint. The wide spectrum of IG applicability includes much-needed new disciplines, such as machine learning [1]. Even more intriguingly, statistical manifolds (SMs) were studied using IG. Figure1 illustrates a statistical manifold $SM(\theta)$ [2], $\theta \in \mathbb{R}^n$.
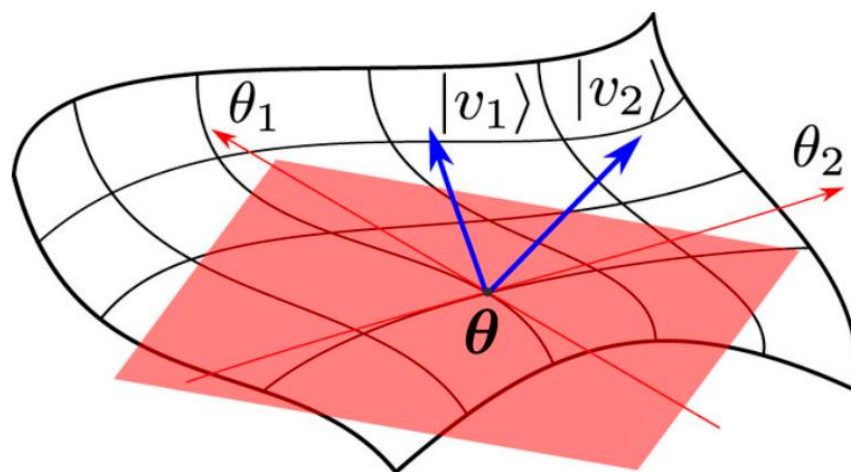

Figure 1: (c.f., [2]).

In this context, IG is a geometric methodology used to analyze models and visualize geometry. It involves studying statistical manifolds, which are defined by probability measurements. The Fisher information metric (FIM) is a key concept in IG, representing a smooth statistical manifold that quantifies the informative difference between measurements [3,4].

The current exposition establishes the first- time ever revolutionary HTBFC info-geometric analysis. The real motivation behind this current innovative study is based on the provided probabilistic distribution of human response time [5]. This drives our creative line of investigation into the reimagining of IG-connected Human-Machine Interactions (HMIs).

This paper's mind map reads: Section II provides IG definitions.

Section III provides a summary of the HTBFC's historical background. The primary results are presented in Section IV by calculating FIM, its inverse, and the FIM of the HTBFC. Section V highlights the important contribution that HTBFC has made to the advancement of robotics. In conclusion, Section VI includes next phase research as well as a few difficult unsolved challenging open problems.

2. Definitions
Definition 1 [6]

1. $M=\{p(x,\theta)|\theta\epsilon\Theta\}$ is SM with a probability density function $p(x,\theta)$ and coordinates, $(\theta_1,\theta_2,..,\theta_n)\epsilon\Theta$.
2. $\Theta=\{p_\theta|\theta\epsilon\Theta\}$ is given by

$$C(x) + \sum_i F_i - \Psi(\theta) = ln\big(p(x;\theta)\big) = \mathcal{L}(x;\theta) \tag{1}$$

$M=\{\mathcal{L}(x;\theta)|\ \theta=(\theta_1,\theta_2,\ldots,\theta_n)\epsilon\mathbb{R}^n\}$ is a manifold.

Definition 2 [6]. $\Psi(\theta)$ (c.f.,Eqn (1)) Define the n-free component of $(-\mathcal{L}(x;\theta))$ containing $(\theta_1,\theta_2,\ldots,\theta_n)$.

Definition 3 [7]. FIM, namely $[g_{ij}]$ reads as

$$[g_{ij}] = \left[\frac{\partial^2}{\partial\theta^i\,\partial\theta^j}\big(\Psi(\theta)\big)\right], i,j = 1,2,\ldots,n \tag{2}$$

Definition 4[8]. $[g^{ij}]$ reads:

$$[g^{ij}] = \big([g_{ij}]\big)^{-1} = \frac{adj[g_{ij}]}{\Delta}, \Delta = \det[g_{ij}] \neq 0 \tag{3}$$

3. The Information Geometrics of the HTBFC
A. Background: HCIs and HTBFC
There is a great need for humans to supervise and intervene in automated systems despite technological advancements. Therefore, future HMIs will require efficient coordination, and emphasize the importance of human trust in automation to achieve this coordination [9-13].

HTBFC is crucial in interactions with automation. To improve this interaction, the user interface can be augmented with more information, which is called automation transparency. Higher levels of transparency increase access to information and help in decision making, leading to an increase in trust. However, high transparency also increases workload and may lead to fatigue that reduces performance. Therefore, for optimal or nearly ideal

performance, adaptive automation should vary based on workload - human trust variations utilizing a dynamic model of human behavior implemented through control rules [14-17].

Researchers have studied human behavior and developed models of trust, showing that transparency influences both trust and workload. However, there is currently no model that can sufficiently detect how human behaviour regarding workload and trust are dynamically impacted by automation transparency. This gap needs to be addressed for control policies based on changes in transparency to improve interactions between humans and machines [18,19]. Figure 2 illustrates a trust-based feedback control approach that uses automation transparency to improve context-specific performance targets during HMIs [5].
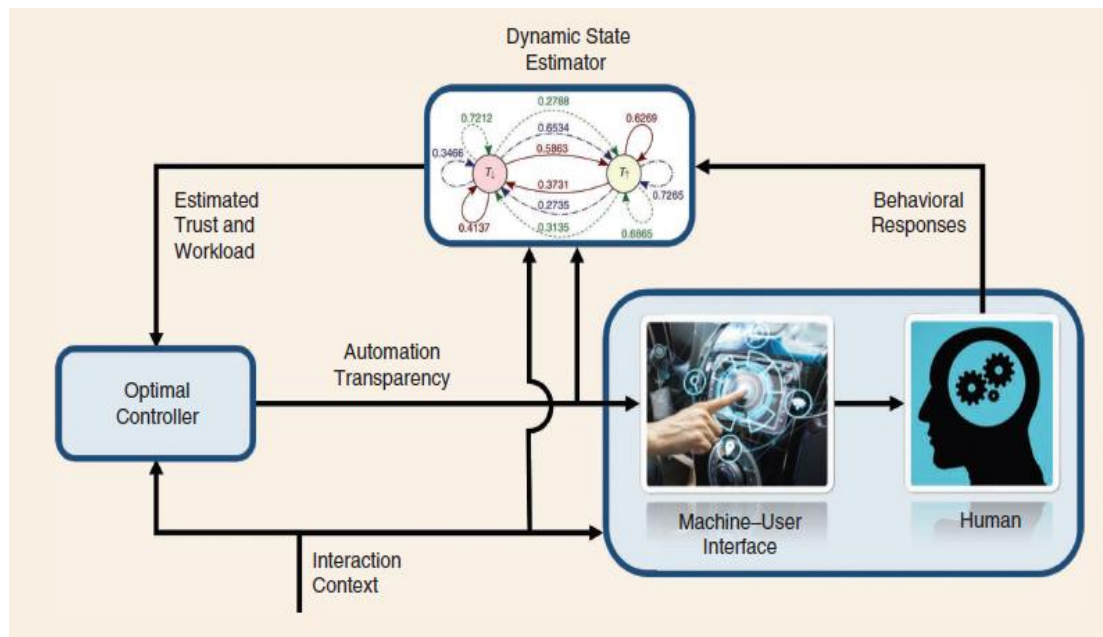
Figure 2: A diagram that shows how humans and machines interact with each other [5].

The importance of human trust in automation is demonstrated by its influence on overall performance [5]. Lack of trust or over trust can lead to negative consequences, so it's important to calibrate human trust for optimal interactions with machines. The article presents a framework that uses probabilistic modeling and behavioral data to adjust the amount and utility of information provided by automation based on human workload dynamics. This approach has been experimentally validated with positive results, suggesting that dynamically updating transparency levels can optimize team performance in real-time adaptive automation systems for humans interacting with intelligent decision aid systems.

The authors of have explored response time and how it is analyzed in experimental psychology [5]. Response time refers to the duration between a stimulus being presented and a human's response, which can vary from trial to trial for the same person. The positively skewed unimodal structure of the response time distribution makes it impossible to represent it as a Gaussian distribution using just mean and variance. However, one of the most common distributions is an exponentially modified Gaussian (ex-Gaussian) distribution (c.f., figure 3), which is formed by mixing an exponential and Gaussian component. Standard distributions such as gamma or log-normal have also been utilized in literature.
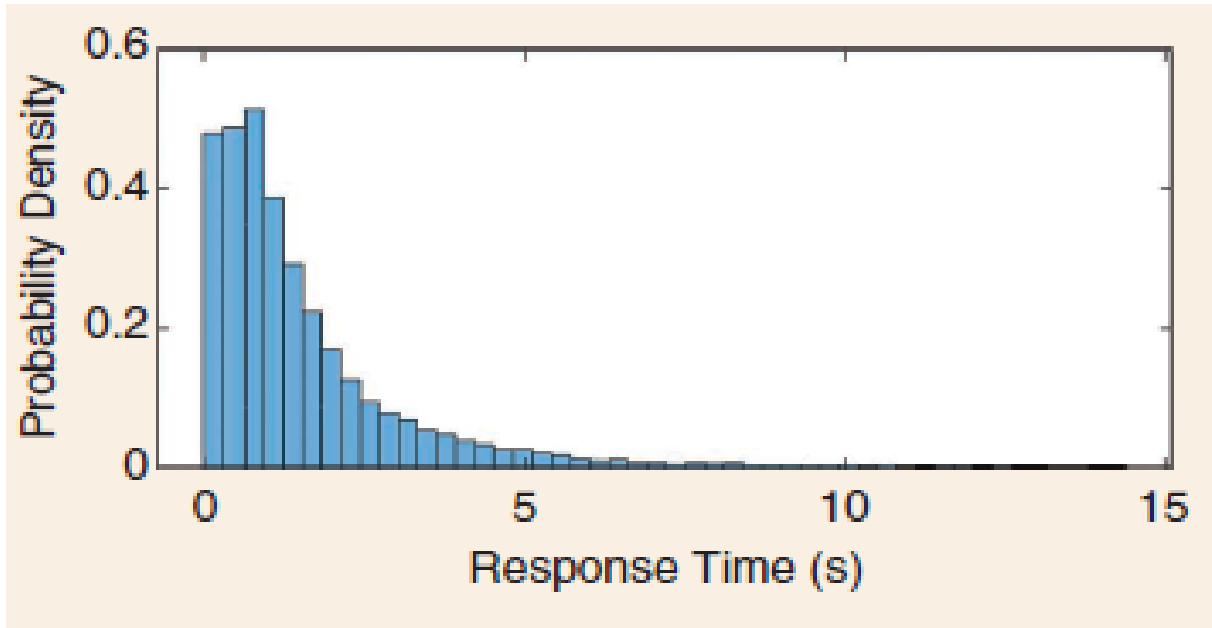
Figure 3: The shape of a response time distribution, which is used to measure how long it takes for humans to respond to stimuli [5]. The distribution has a skewed, bell-shaped curve with most responses occurring quickly and fewer taking longer- times.

The ex-Gaussian distribution is a statistical model used to describe human response time [5]. The distribution has three parameters: μ, σ and τ represent the average and a Gaussian component's standard deviation. In this paper, τ defines the decay rate of an exponential component, with $\sigma, \tau > 0$. Researchers have attributed these components to decision-making processes and residual processes in humans, but this idea remains unproven. However, it is discovered that the ex-Gaussian distribution fits response time data more accurately than other distributions, such as the gamma or log-normal distributions. Having defined $\sigma, \tau > 0$, the ex-Gaussian distribution is characterized by the probability density function:

$$p(x) = \frac{1}{2\tau} \exp\left(\frac{\sigma^2}{2\tau^2} - \frac{x-\mu}{\tau}\right) erfc\left(\frac{\sigma^2}{\tau} - (x-\mu)\right) \tag{4}$$

erfc Serves as the complementary error function:

$$erfc(x) = \int_0^\infty e^{-z^2} \, dz \tag{5}$$

Notably, the Chernoff-Type Bounds for the Gaussian Error Function *erfc* [20] is given by the inequality:

$$erfc(x) \geq \sqrt{\frac{2e}{\pi}} \, \frac{\sqrt{\beta-1}}{\beta} \, e^{-\beta x^2}, x \geq 0, \beta > 1 \tag{6}$$

With e to serve as Euler–Mascheroni constant,

4. The Information Geometrics of the HTBFC Manifold
Theorem 1 HTBFC Manifold of (4) and (6), satisfies:
(i)FIM reads as

$$[g_{ij}] = \begin{pmatrix} a & f & g & h & 0 \\ f & b & r & s & 0 \\ g & r & c & v & 0 \\ h & s & v & d & 0 \\ 0 & 0 & 0 & 0 & m \end{pmatrix} \tag{7}$$

Where

$$a = 2\beta\left(\frac{3\sigma^4}{\tau^4} + \frac{2\mu\sigma^2}{\tau^3}\right) - \left(\frac{1}{\tau^2} + \frac{6\sigma^2}{\tau^4} + \frac{2\mu}{\tau^3}\right) \tag{8}$$

$$f = \frac{4\sigma}{\tau^3} - 4\beta\left(\frac{2\sigma^3}{\tau^3} + \frac{\mu\sigma}{\tau^2}\right) \tag{9}$$

$$g = \frac{1}{\tau^2}(1 - 2\beta\sigma^2) \tag{10}$$

$$h = -2\frac{\sigma^2}{\tau^3}(\sigma^2 + \mu\tau) \tag{11}$$

$$b = 4\beta\left(\frac{3\sigma^2}{\tau^2} + \frac{\mu}{\tau}\right) - \frac{4\sigma}{\tau^2} \tag{12}$$

$$r = \frac{4\sigma\beta}{\tau} \tag{13}$$

$$s = \frac{4\sigma^3}{\tau^2} + 4\frac{\mu\sigma}{\tau} \tag{14}$$

$$c = 2\beta \tag{15}$$

$$v = 2\mu + \frac{2\sigma^2}{\tau} \tag{16}$$

$$d = -\frac{1}{\beta^2} \tag{17}$$

$$m = \frac{1}{\lambda^2} \tag{18}$$

(ii) $[g_{ij}]^{-1}$ Takes the form

$$[g^{ij}] = ([g_{ij}])^{-1} = \frac{1}{\Delta}[C^T], \Delta \neq 0 \tag{19}$$

Where Δ is the determinant of $[g_{ij}]$, C is the matrix of cofactors of g^{ij}, and C^T represents the matrix transpose.

- **Proof**

We have

$$p(x) = \frac{1}{2\tau}\exp\left(\frac{\sigma^2}{2\tau^2} - \frac{x-\mu}{\tau}\right) erfc\left(\frac{\sigma^2}{\tau} - (x-\mu)\right) \text{(c.f., (4))}$$

Thus, it follows that:

$$\mathcal{L}(x;\theta) = ln\big(p(x;\theta)\big)$$

$$= \left(-ln2 - \ln\tau + \left(\frac{\sigma^2}{2\tau^2} - \frac{x-\mu}{\tau}\right) + ln\, erfc\left(\frac{\sigma^2}{\tau} - (x-\mu)\right)\right) \tag{20}$$

Following (6), we can re-write

$$erfc\left(\frac{\sigma^2}{\tau} - (x-\mu)\right) = \lambda\sqrt{\frac{2e}{\pi}}\,\frac{\sqrt{\beta-1}}{\beta}\,e^{-\beta\left(\frac{\sigma^2}{\tau} - (x-\mu)\right)^2} \tag{21}$$

Such that $x \geq 0, \lambda \geq 1, \beta > 1$

Therefore,

$$\mathcal{L}(x;\theta) = ln\big(p(x;\theta)\big)$$

$$= -ln2 - ln\,\tau + \left(\frac{\sigma^2}{2\tau^2} - \frac{x-\mu}{\tau}\right) + ln\,\lambda + ln\left(\sqrt{\frac{2e}{\pi}}\right) + \frac{1}{2}l\,n(\beta-1) - ln\beta - \beta\left(\frac{\sigma^2}{\tau} - (x-\mu)\right)^2 \quad (22)$$

To this end, we obtain $\Psi(\theta)$ reads as:

$$\Psi(\theta) = ln2 + ln\,\tau + \left(\frac{\sigma^2}{2\tau^2} + \frac{\mu}{\tau}\right) - ln\,\lambda - ln\left(\sqrt{\frac{2e}{\pi}}\right) - \frac{1}{2}l\,n(\beta-1) + ln\beta + \beta\left(\frac{\sigma^4}{\tau^2} + \mu^2 + \frac{2\mu\sigma^2}{\tau}\right) \quad (23)$$

$$\theta = (\theta_1, \theta_2, \theta_3, \theta_4, \theta_5) = (\tau, \sigma, \mu, \beta, \lambda)$$

We have

$$\partial_1 = \frac{\partial\Psi}{\partial\tau} = [\frac{1}{\tau} + \frac{2\mu\sigma^2}{\tau^3} + \frac{\mu}{\tau^2} - \frac{2\beta\sigma^2}{\tau^3}(\sigma^2 + \mu\tau)] \quad (24)$$

$$\partial_2 = \frac{\partial\Psi}{\partial\sigma} = [-\frac{2\sigma}{\tau^2} + 4\beta\frac{\sigma}{\tau^2}(\sigma^2 + \mu\tau\sigma \quad (25)$$

$$\partial_3 = \frac{\partial\Psi}{\partial\mu} = -\frac{1}{\tau} + 2\beta\left(\frac{\sigma^2}{\tau} + \mu\right) \quad (26)$$

$$\partial_4 = \frac{\partial\Psi}{\partial\beta} = \frac{1}{\beta} + (\frac{\sigma^4}{\tau^2} + \frac{2\mu\sigma^2}{\tau} + \mu^2) \quad (27)$$

$$\partial_5 = \frac{\partial\Psi}{\partial\lambda} = -\frac{1}{\lambda} \quad (28)$$

$$\partial_1\partial_1 = 2\beta(\frac{3\sigma^4}{\tau^4} + \frac{2\mu\sigma^2}{\tau^3}) - (\frac{1}{\tau^2} + \frac{6\sigma^2}{\tau^4} + \frac{2\mu}{\tau^3}) \quad (\text{c.f., (8)})$$

$$\partial_1\partial_2 = \frac{4\sigma}{\tau^3} - 4\beta\left(\frac{2\sigma^3}{\tau^3} + \frac{\mu\sigma}{\tau^2}\right) = \partial_2\partial_1 \quad (\text{c.f., (9)})$$

$$\partial_1\partial_3 = \partial_3\partial_1 = \frac{1}{\tau^2}(1 - 2\beta\sigma^2) \quad (\text{c.f., (10)})$$

$$\partial_1\partial_4 = \partial_4\partial_1 = -2\frac{\sigma^2}{\tau^3}(\sigma^2 + \mu\tau) \quad (\text{c.f., (11)})$$

$$\partial_1\partial_5 = \partial_5\partial_1 = \partial_2\partial_5 = \partial_5\partial_2 = \partial_3\partial_5 = \partial_5\partial_3 = \partial_4\partial_5 = \partial_5\partial_4 = 0 \quad (29)$$

$$\partial_2\partial_2 = 4\beta\left(\frac{3\sigma^2}{\tau^2} + \frac{\mu}{\tau}\right) - \frac{4\sigma}{\tau^2} \quad (\text{c.f.,(12)})$$

$$\partial_2\partial_3 = \partial_3\partial_2 = \frac{4\sigma\beta}{\tau} \quad (\text{c.f.,(13)})$$

$$\partial_2\partial_4 = \partial_4\partial_2 = \frac{4\sigma^3}{\tau^2} + 4\frac{\mu\sigma}{\tau} \quad (\text{c.f.,(14)})$$

$$\partial_3\partial_3 = 2\beta \quad (\text{c.f., (15)})$$

$$\partial_3\partial_4 = \partial_4\partial_3 = 2\mu + \frac{2\sigma^2}{\tau} \quad (\text{c.f., (16)})$$

$$\partial_4\partial_4 = -\frac{1}{\beta^2} \quad (\text{c.f., (17)})$$

$$\partial_5\partial_5 = \frac{1}{\lambda^2} \quad (\text{c.f., (18)})$$

Hence, FIM (c.f., (i)) follows.
(ii) Follows by the definition of Inverse matrices.

Now, we are going to provide examples for both two- and three-dimensional cases.

• **The Two-Dimensional Case**
Due to the higher complexity of the mathematical calculations of $[g^{ij}]$ (c.f., (19)), it is more favorable to explore the two-dimensional special case.
Let $\tau = \lambda = 1, \beta = 2$. this reduces the generated potential function, $\Psi(\theta)$ (c.f., (23)) to take the form:

$$\Psi(\theta) = 2ln2 + \left(\frac{\sigma^2}{2} + \mu\right) - ln\left(\sqrt{\frac{2e}{\pi}}\right) + 2\left(\sigma^4 + \mu^2 + 2\mu\sigma^2\right) \tag{30}$$

This implies:

$$\partial_1 = \sigma + 8\sigma^3 + 8\mu\sigma \tag{31}$$

$$\partial_2 = 1 + 4\mu + 4\sigma^2 \tag{32}$$

$$\partial_1\partial_1 = 1 + 24\sigma^2 + 8\mu \tag{33}$$

$$\partial_1\partial_2 = 8\sigma = \partial_2\partial_1 \tag{34}$$

$$\partial_2\partial_2 = 4 \tag{35}$$

Consequently,

$$[g_{ij}] = \begin{pmatrix} 1 + 24\sigma^2 + 8\mu & 8\sigma \\ 8\sigma & 4 \end{pmatrix} \tag{36}$$

Thus, the determinant of $[g_{ij}]$, Δ will be given by

$$\Delta = 4(1 + 8\mu + 8\sigma^2) \tag{37}$$

So, $\Delta = 0$ if and only if

$$1 + 8\mu + 8\sigma^2 = 0 \tag{38}$$

Which is impossible, since both μ and σ are pre-defined to be positive. This demonstrates that $[g^{ij}]$ exists.
Following some mathematical steps, it can be verified that:

$$[g^{ij}] = \frac{1}{\Delta}\begin{pmatrix} 4 & -8\sigma \\ -8\sigma & 1 + 24\sigma^2 + 8\mu \end{pmatrix}$$

• **The Three-Dimensional Case**
Moving to the three-dimensional configuration, for example, putting $\sigma = 1$ and $\beta = 2$ (c.f., (23)), it follows that:

$$\Psi(\theta) = 2\,ln2 + ln\,\tau + \left(\frac{1}{2\tau^2} + \frac{\mu}{\tau}\right) - ln\,\lambda - ln\left(\sqrt{\frac{2e}{\pi}}\right) + 2\left(\frac{1}{\tau^2} + \mu^2 + \frac{2\mu}{\tau}\right) \tag{40}$$

$$\theta = (\theta_1, \theta_2, \theta_3) = (\tau, \mu, \lambda)$$

In analogy to the above proofs, it can be easily shown that the three-dimensional generated HTBFC manifold is characterized by

$$[g_{ij}] = \begin{pmatrix} \frac{1}{\tau^4}(3 + 8\tau - \tau^2) & 0 & 0 \\ 0 & 4 & 0 \\ 0 & 0 & \frac{1}{\lambda^2} \end{pmatrix} \tag{41}$$

Provided that:

$$\Delta = \det([g_{ij}]) = \frac{4}{\lambda^2\tau^4}(3 + 8\tau - \tau^2) \tag{42}$$

This triggers a new breakthrough:
What are the values of the three-dimensional vector (τ,μ,λ) to guarantee the existence of the inverse FIM matrix, $[g^{ij}]$?
To answer this triggering question, set $\Delta=0$
Consequently, it is implied that:

$$\frac{4}{\lambda^2\tau^4}(3 + 8\tau - \tau^2) = 0 \tag{43}$$

Hence,

$$\tau \rightarrow \infty, \text{ or } \lambda \rightarrow \infty \tag{44}$$

or

$$(3 + 8\tau - \tau^2) = 0 \tag{45}$$

By (45), $\tau>0$, we have

$$\tau = 4 + \sqrt{19} \tag{46}$$

Therefore, $[g^{ij}]$ will exist if and only if

$$\tau \neq 4 + \sqrt{19}, \ \tau, \mu, \text{ and } \lambda \text{ are positive real numbers} \tag{47}$$

Thus, $[g^{ij}]$ will take the form:

$$[g^{ij}] = \frac{1}{\Delta} \begin{pmatrix} \frac{4}{\lambda^2} & 0 & 0 \\ 0 & \frac{1}{\lambda^2\tau^4}(3 + 8\tau - \tau^2) & 0 \\ 0 & 0 & \frac{4}{\tau^4}(3 + 8\tau - \tau^2) \end{pmatrix} \tag{48}$$

with Δ(c.f., (42) and (47)).

Based on the above analysis, $[g^{ij}]$ always exists in the two-dimensional case, whereas its existence is constrained by $\tau \neq 4 + \sqrt{19}$, τ,μ, and λ are positive real numbers. It is expected that the four-dimensional case will impose more restrictions to the existence of [g^ij].

5. HTBFC Applications to Robotics
Researchers ran an experiment where participants engaged with a simulation comprising numerous reconnaissance missions to better understand HTBFC and workload in a decision-aid system [16]. Participants had to search buildings to assess their level of safety or danger based on the presence of armed men. To maximize both speed and safety, a decision-assistance robot made suggestions regarding whether to wear light or heavy armor during the hunt. The study examined the effects of various system transparency levels on user workload, performance, and human-robot interaction trust.

Participants were helped by a robot that varied in transparency during each mission of the experiment [16]. The low transparency robot suggested Armor and disclosed whether there were any armed

assailants. As figure 4 [16] illustrates, it is crucial to remember that various degrees of transparency might change according to automation, context, and viability.


Figure 4: Screenshots of robot reports with varying levels of transparency.

The participants completed the six trials that made up the instructional mission before the main experiment started so they could get acquainted with the three degrees of transparency and the research interface. Every participant was assigned the identical lesson task. To mitigate potential biases and the impact of variables like task completion order, participants were randomised to the missions for every transparency level.

As part of the study, participants had to evaluate robot reports on whether there were shooters inside a facility. Seventy percent of the time, the robot's suggestions were accurate, and the errors were either misses or false alarms, see figure 5(c.f., [16]).
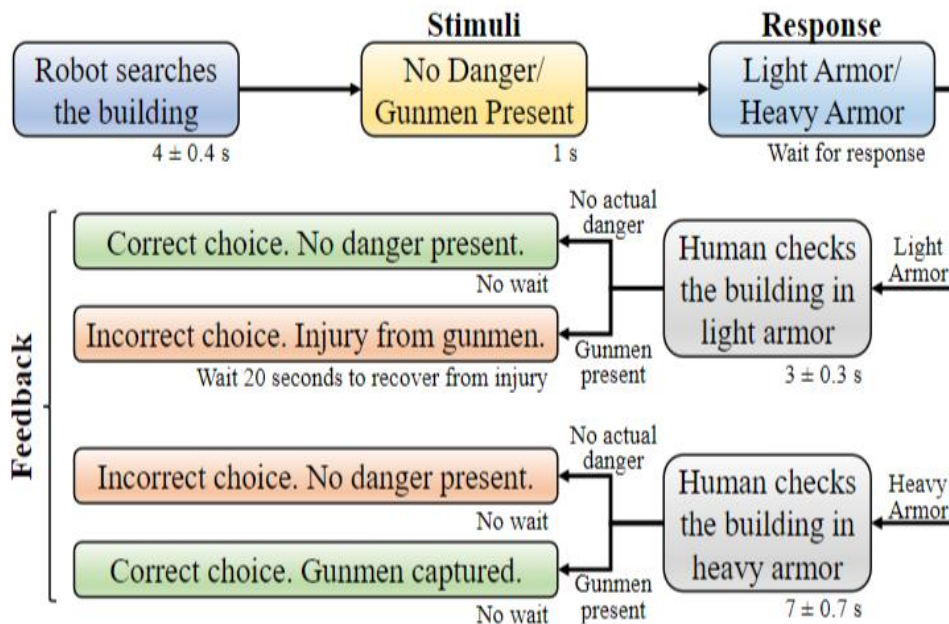
Figure 5: The displayed information is relevant for understanding the timing and presentation of data during the trial, providing insights into the experimental setup and the temporal aspects of the study.

Most existing trust models in human-robot interaction (HRI) are designed for specific types of interactions or robotic agents, making it difficult to compare their accuracy [21]. This calls for the creation of a general HRI trust model that can be used in a variety of robotic domains, doing away with the necessity to create unique models of trust for each one.

Within HRI's domain, trust is a multifaceted notion that can be divided into two categories: relation-based trust and performance-based trust [22-24]. A more encompassing definition of trust is required since current definitions from other domains do not adequately convey the multifaceted nature of trust within HRI.

Additionally, while there are studies on trust violation and repair, there is a need for research exploring the dynamics of trust loss and repair over time, particularly in relation to different types of failures and trust repair strategies. This raises issues about the efficacy of trust-repair techniques in long-term interactions as well as the effect of growing accustomed to a robotic agent on trust loss resulting from robot failure [22-24]. Additionally, it draws attention to the dearth of trust models that are currently available and applicable to a variety of robotic activities and domains, which makes it more difficult to assess and contrast trust models. Notably, this suggests the potential use of trust measurement methods from other fields,

such as psychology and sociology, to accurately assess trust in human-robot interaction and develop trust models independent of various influencing factors.

Existing trust models in HRI are often specific to certain types of interactions, tasks, or robotic agents, making them difficult to compare or apply to different domains [22-24]. This lack of a general trust model hinders the evaluation and development of trust models in HRI. It would be unnecessary to develop new models for every new robotic activity if there was a universal trust model that could be used across different robotic activities and domains. Many disciplines, including psychology, sociology, and physiology, are interested in the concept of trust. In these domains, trust is measured using a variety of indicators, including objective evaluations like trust games and physiological measurements. By using these measurement techniques, trust in HRI can be assessed more accurately, circumventing the drawbacks of existing techniques, and aiding in the development of trust models that are not influenced by a variety of variables.

6. Conclusions and Future Work
The goal of the current study is to use robust IG methods to assess HTBFC info-geometrically. To enable relativistic analysis of its linked manifold and to offer fresh, imaginative insights into HTBFC

performance, IG is included into HTBFC theory.

This current study's arising open problems are:
- How feasible is it to calculate the inverse FIM (c.f., (19)) in four dimensions?
- Having solved open problem 1, can we proceed with this revolutionary IG analysis to obtain the exact form of $[g^{ij}]$ (c.f., (19)) for the five-dimensional HTBFC manifold?
- Assuming the solvability of open problem 2, is it possible to employ this influential IG approach to analyse the dynamics of Human- Driven vehicles?
- Future research pathways include finding answers to these open problems.

Refrences

1. Mageed, I. A., Zhou, Y., Liu, Y., & Zhang, Q. (2023, August). Towards a Revolutionary Info-Geometric Control Theory with Potential Applications of Fokker Planck Kolmogorov (FPK) Equation to System Control, Modelling and Simulation. In *2023 28th International Conference on Automation and Computing (ICAC)* (pp. 1-6). IEEE.
2. [Belliardo, F., & Giovannetti, V. (2021). Incompatibility in quantum parameter estimation. *New Journal of Physics, 23*(6), 063055.
3. S. Eguchi, S., & Komori, O. (2022). Minimum Divergence Methods in Statistical Machine Learning.
4. I. Mageed, I. A., Zhang, Q., Akinci, T. C., Yilmaz, M., & Sidhu, M. S. (2022, October). Towards Abel Prize: The Generalized Brownian Motion Manifold's Fisher Information Matrix With Info-Geometric Applications to Energy Works. In *2022 Global Energy Conference (GEC)* (pp. 379-384).
5. XYang, X. J., Schemanske, C., & Searle, C. (2021). Toward quantifying trust dynamics: How people adjust their trust after moment-to-moment interaction with automation. *Human Factors, 65*(5), 862-878.
6. Kondor, R., & Trivedi, S. (2018). On the generalization of equivariance and convolution in neural networks to the action of compact groups. In *International conference on machine learning* (pp. 2747-2755). PMLR.
7. A. Mageed, X. Yin, Y. Liu and Q. Zhang. (2023). "Z(a,b) of the Stable Five-Dimensional M/G/1 Queue Manifold Formalism's Info- Geometric Structure with Potential Info-Geometric Applications to Human Computer Collaborations and Digital Twins. *28th International Conference on Automation and Computing (ICAC),* Birmingham, United Kingdom, 2023, pp. 1-6.
8. Mageed, I. A., & Kouvatsos, D. D. (2021, February). The Impact of Information Geometry on the Analysis of the Stable M/G/1 Queue Manifold. In *ICORES* (pp. 153-160).
9. Kousi, N., Dimosthenopoulos, D., Aivaliotis, S., Michalos, G., & Makris, S. (2022). Task allocation: Contemporary methods for assigning human–robot roles. The 21st Century Industrial Robot: When Tools Become Collaborators, 215-233.
10. Soga, L. R., Vogel, B., Graça, A. M., & Osei-Frimpong, K. (2021). Web 2.0-enabled team relationships: An actor-network perspective. *European Journal of Work and Organizational Psychology, 30*(5), 639-652.
11. Simon, L., Guérin, C., Rauffet, P., Chauvin, C., & Martin, É. (2023). How humans comply with a (potentially) faulty robot: Effects of multidimensional transparency. *IEEE Transactions on Human-Machine Systems.*
12. Lee, J. D., & See, K. A. (2004). Trust in automation: Designing for appropriate reliance. *Human factors, 46*(1), 50-80.
13. Sheridan, T. B., & Parasuraman, R. (2005). Human-automation interaction. *Reviews of human factors and ergonomics, 1*(1), 89-129.
14. Skraaning, G., & Jamieson, G. A. (2021). Human performance benefits of the automation transparency design principle: Validation and variation. *Human factors, 63*(3), 379-401.
15. O'Neill, T., McNeese, N., Barron, A., & Schelble, B. (2022). Human–autonomy teaming: A review and analysis of the empirical literature. *Human factors, 64*(5), 904-938.
16. Akash, K., McMahon, G., Reid, T., & Jain, N. (2020). Human trust-based feedback control: Dynamically varying automation transparency to optimize human-machine interactions. *IEEE Control Systems Magazine, 40*(6), 98-116.
17. Han, L., Du, Z., Wang, S., & Chen, Y. (2022). Analysis of traffic signs information volume affecting driver's visual characteristics and driving safety. *International journal of environmental research and public health, 19*(16), 10349.
18. Akash, K., Polson, K., Reid, T., & Jain, N. (2019). Improving human-machine collaboration through transparency-based feedback–part I: Human trust and workload model. *IFAC-PapersOnLine, 51*(34), 315-321.
19. Akash, K., Reid, T., & Jain, N. (2019). Improving human-machine collaboration through transparency-based feedback–part ii: Control design and synthesis. *IFAC-PapersOnLine, 51*(34), 322-328.
20. Han, Q., & Kato, K. (2022). Berry–Esseen bounds for Chernoff-type nonstandard asymptotics in isotonic regression. *The Annals of Applied Probability, 32*(2), 1459-1498.
21. Khavas, Z. R., Ahmadzadeh, S. R., & Robinette, P. (2020). Modeling trust in human-robot interaction: A survey. In *International conference on social robotics* (pp. 529-541). Cham: Springer International Publishing.
22. Khavas, Z. R. (2021). A review on trust in human-robot interaction.
23. Wang, Q., Liu, D., Carmichael, M. G., Aldini, S., & Lin, C. T. (2022). Computational model of robot trust in human co-worker for physical human-robot collaboration. *IEEE Robotics and Automation Letters, 7*(2), 3146-3153.
24. Aldini, S., Akella, A., Singh, A. K., Wang, Y. K., Carmichael, M., Liu, D., & Lin, C. T. (2019). Effect of mechanical resistance on cognitive conflict in physical human-robot collaboration. In *2019 international conference on robotics and automation (ICRA)* (pp. 6137-6143). IEEE.